Available online at www.sciencedirect.com
ScienceDirect
Journal of Molecular Catalysis A: Chemical 271 (2007) 238–245
JOURNAL OF MOLECULAR CATALYSIS A: CHEMICAL
www.elsevier.com/locate/molcata

Nature of cobalt active species in hydrodesulfurization catalysts: Combined support and preparation method effects

A.M. Venezia [a,*], R. Murania [b], G. Pantaleo [b], G. Deganello [a,b]

[a] *Istituto dei Materiali Nanostrutturati (ISMN-CNR) via Ugo La Malfa, 153, Palermo I-90146, Italy*
[b] *Dipartimento di Chimica Inorganica ed Analitica "Stanislao Cannizzaro", Università di Palermo, Viale delle Scienze, Parco d'Orleans, Palermo I-90128, Italy*

Received 3 January 2007; received in revised form 24 February 2007; accepted 24 February 2007
Available online 28 February 2007

Abstract

Co/γ-Al_2O_3, Co/SiO_2, Co/MCM-41, Co/ASA and Co/S2 (amorphous aluminosilicate with Al/Si = 0.13 and with Al/Si ≈ 2, respectively) were prepared by the method of wet impregnation and by the method of precipitation in the presence of sodium carbonate. The samples were characterised by XPS, XRD and TPR. The catalytic activity was tested in the hydrodesulfurization of thiophene using a continuous flow reactor. Among the wet impregnated catalysts those supported on the amorphous and ordered mesoporous silica exhibited higher HDS activity as compared to the alumina containing supports. Particularly, the use of the mesoporous, high surface area MCM-41 support, determined the best performing cobalt catalyst. Quite surprisingly, the catalytic performance of the cobalt catalysts was completely reversed by using the method of precipitation with sodium carbonate. In this case the alumina supported catalyst was the most active. For the wet impregnated samples, the positive influence of SiO_2, as compared to the aluminosilicates, was related to the formation of Co_3O_4 which on the other supports was hindered by the interaction with alumina. On the contrary, using the method of precipitation with sodium carbonate, Co_3O_4 formed on the alumina containing supports, whereas cobalt-support interacting species formed over the two types of SiO_2. Increased cobalt reducibility and cobalt dispersion accounted for the different catalytic behaviour.

Keywords: Co catalysts; HDS; Co_3O_4; Support effect; Mesoporous MCM-41

1. Introduction

The recent environmental legislation that limits the amount of sulfur in gas oils and Diesel fractions to less than 50 ppm, drives a growing interest in developing highly active catalysts for hydrodesulfurization (HDS) [1]. The commercially used alumina supported CoMo catalysts have good performance and economic advantage. However, under the severe conditions of high temperature and pressure, needed to desulfurize the most refractory alkyl substituted dibenzothiopenes, these catalysts are deactivated by the processes of sintering and/or coke formation [2]. Early investigation on the role of the cobalt on the hydrodesulfurization activity of the CoMo systems resulted in different structural models such as the intercalation model [3], the contact synergy model [4] and the CoMoS model in which cobalt was demonstrated to decorate the edges of MoS_2 slabs [2,5]. In all of these structures Co was considered the promoter of the Mo activity. A different approach based on the experimental observation that Co/C catalysts exhibited higher HDS activities than Mo/C catalysts, regarded the cobalt as the active species and Mo as structural promoter of the CoMo systems [6]. The use of monometallic cobalt catalysts is widely described in literatures [7,8]. The catalytic performance is related to the preparation methods, the type of supports and the loading of the cobalt [7,9,10]. Indeed all of the above-mentioned aspects influence the final catalyst dispersion and also the reducibility of the metal. In other words they affect the morphology and the electronic structure of the active species.

A recent study, from this laboratory, on CoMo catalysts supported on sol–gel prepared oxides with different Al/Si ratio, going from pure silica to pure alumina, has indicated better HDS performance for the alumina supported catalyst as compared to

* Corresponding author. Fax: +39 0916809399.
E-mail address: anna@pa.ismn.cnr.it (A.M. Venezia).

1381-1169/$ – see front matter © 2007 Elsevier B.V. All rights reserved.
doi:10.1016/j.molcata.2007.02.039

the silica one and a maximum of activity in correspondence of Al/Si ≈ 2 [11]. The effect of the specific composition of the mixed support was attributed to different strength and polarizability of Mo–O–Al or Mo–O–Si links responsible for the final dispersion and reducibility of the Mo [11,12]. However, the study did not focus on the effect of cobalt and of possible Co–support interaction. In order to understand the role of cobalt and aiming to obtain new HDS catalysts with improved performance, the present report describes the activity–structure relationship of a series of cobalt catalysts supported on silica, amorphous and ordered mesoporous MCM-41, alumina and mixed aluminosilicate, tested in the HDS reaction of thiophene. Two different methods of synthesis are used aiming to achieve different degree of metal–support interaction and to possibly control the active phase dispersion.

2. Experimental

2.1. Supports and catalyst preparation

The aluminosilicate support indicated as S2 was prepared by sol–gel route according to the previously described procedure [13]. The composition of 50/50 of silica/alumina was chosen on the basis of the previous study showing the positive effect of such support on the HDS activity of the CoMo catalyst [11]. The MCM-41 was prepared by hydrothermal method according to the method reported by Choma et al. [14]. The surfactant, hexadecyl trimethylammoniumbromide (CTAB), was dissolved in a solution of aqueous ammonia (28 wt.%), distilled water and ethanol. After stirring this mixture for 10 min, the tetraethoxysylane (TEOS) was added. The molar composition of the gel was: 0.09 TEOS:1.12 NH_4OH:4.86 EtOH:0.04 CTAB:15.62 H_2O. This mixture was homogenized by stirring for 2 h at ambient temperature before heating at 100 °C for a total of 5 days under static conditions. Thereafter the product was calcined at 650 °C for 6 h in air. Attainment of the ordered mesoporous structure was confirmed by the XRD pattern showing the typical reflection at $2\theta \approx 2^\circ$ and by the typical type IV N_2 adsorption–desorption isotherm [15,16]

A series of catalysts, containing 5 wt.% Co, was prepared by incipient wetness impregnation (wi), involving impregnation of the synthetic S2 support, SiO_2 (amorphous silica gel 60, Merck), siliceus MCM-41, amorphous silicate (ASA) (Aldrich) and γ-Al_2O_3 (Aldrich) with an aqueous solution of $Co(NO_3)_2{\cdot}6H_2O$ followed by 2 h drying at 120 °C and calcination at 400 °C for 2 h. Another series, also with 5 wt.% Co, was prepared by precipitation of cobalt hydroxide on the support. The procedure consisted in adding slowly a 1 M solution of Na_2CO_3 (pH 10) to the suspension of the support in aqueous cobalt nitrate. The suspension was stirred at room temperature for 1 h and then the solid was filtered and washed to eliminate the sodium ions. Thereafter the solid was dried at 120 °C overnight and calcined at 400 °C for 4 h. The Co loading was checked by X-ray fluorescence analyses. In the sample notation, the supports and the preparation methods as *wi* for wet impregnated and *carb*. for the Na_2CO_3 precipitated catalysts, are indicated.

2.2. Catalyst characterization

2.2.1. X-ray diffraction

X-ray diffraction measurements for the structure determination were carried out with a Philips vertical goniometer using Ni-filtered Cu Kα radiation. A proportional counter and 0.05° step sizes in 2θ were used. The assignment of the various crystalline phases was based on the JPDS powder diffraction file cards [17].

2.2.2. BET analyses

The microstructural characterization was performed with a Carlo Erba Sorptomat 1900 instrument. The fully computerised analysis of the adsorption isotherm of nitrogen at liquid nitrogen temperature, allowed obtaining, through the BET approach, the specific surface area of the samples. By analysis of the desorption curve, using the BJH calculation method, the pore size volume distribution was also obtained [18].

2.2.3. X-ray photoelectron spectroscopy (XPS)

The X-ray photoelectron spectroscopy analyses were performed with a VG Microtech ESCA 3000 Multilab, equipped with a dual Mg/Al anode. The spectra were excited by the unmonochromatised Al Kα source (1486.6 eV) run at 14 kV and 15 mA. The analyser operated in the constant analyser energy (CAE) mode. For the individual peak energy regions, a pass energy of 20 eV set across the hemispheres was used. Survey spectra were measured at 50 eV pass energy. The sample powders were analysed as pellets, mounted on a double-sided adhesive tape. The pressure in the analysis chamber was in the range of 10^{-8} Torr during data collection. The constant charging of the samples was removed by referencing all the energies to the C 1s set at 285.1 eV, arising from the adventitious carbon. The invariance of the peak shapes and widths at the beginning and at the end of the analyses ensured absence of differential charging. Analyses of the peaks were performed with the software provided by VG based on non-linear least squares fitting program using a weighted sum of Lorentzian and Gaussian component curves after background subtraction according to Shirley and Sherwood [19,20]. Atomic concentrations were calculated from peak intensity using the sensitivity factors provided with the software. The binding energy values are quoted with a precision of ±0.15 eV and the atomic percentage with a precision of ±10%. Contact of the samples with air was minimised during sample loading; particular care was adopted for samples analysed after the sulfiding treatment and the HDS reaction. In this case the samples were kept in *n*-heptane until being transferred into the XPS instrument.

2.2.4. Zero point charge determination (ZPC)

The ZPC of the various supports was determined by mass titration [13,21]. According to this method, the variation of pH of a water solution containing increasing amount of solid was monitored until the steady-state value of pH (ZPC) was reached.

2.2.5. Hydrogen temperature programmed reduction (H_2-TPR)

TPR measurements were conducted with a Micromeritics AutoChem 2910 automated catalyst characterization system, equipped with a thermal conductivity detector (TCD). About 0.1 g of sample was used for each measurement. The samples were pre-treated with a mixture of 5 vol.% O_2/He at 50 ml/min, heating up (10 °C/min) to 400 °C and holding at this temperature for 30 min. After lowering the temperature down to 50 °C, the gas mixture of 5 vol.% H_2/Ar was introduced at 30 ml/min into the sample tube and was also used as a reference gas. During the analysis, the temperature was increased up to 1000 °C at a rate of 10 °C/min. The effluent gas was analysed with a TCD.

2.3. HDS reaction

The hydrodesulfurization of thiophene was carried out in the vapour phase using a continuous flow microreactor and according to the procedure described previously [11,22]. An amount of 200 mg of catalyst (sieved fraction 210–430 μm), diluted with inert particles of SiC, was used for each test. The samples were sulfided in situ with a mixture of 10 vol.% H_2S/H_2, at 50 ml/min, while raising the temperature up to 400 °C at a rate of 7 °C/min and were maintained at this temperature for 2 h. After purging with nitrogen, the HDS of thiophene was carried out at 340 °C with 5.3 vol.% thiophene in H_2 and WHSV = 7500 h^{-1}. The reaction products were analysed by on-line gas chromatography (Carlo Erba GC 8340 gaschromatograph). Fractional conversions were calculated from the ratio of the peak area of the C_4 products over the sum of the peak areas of the products and thiophene. The reaction rate for HDS (r_{HDs}) was calculated from the fractional conversion at the steady state conditions, reached after 8 h on stream, assuming a first order reaction in thiophene. Conversions at the beginning of the reaction were also considered in order to determine the initial deactivation. For this purpose a percentage of deactivation defined as $\%d = 100 \times (x_i - x_f)/x_i$ with x_i and x_f being the conversion under initial and stationary conditions was calculated. Measurements of the rate constants at the temperatures of 355, 370 and 395 °C allowed to determine the apparent activation energy for each catalyst [22]. The lack of deactivation was checked by experiment of ascending and descending temperature. The relative error on the catalytic activity data was of the order of 10%.

3. Results and discussion

In Table 1 the catalytic results in terms of thiophene HDS reaction rate, activation energy and % deactivation are reported for the two series of catalysts. For comparison reason two catalysts: Mo (6.4 wt.%)/ASA and Co (1.6 wt.%)Mo (6.4)/ASA are also listed. The histograms of the rate as a function of the catalyst supports and catalyst preparation are reported in Fig. 1. Quite clearly the effect of different supports on the activity of the cobalt catalyst is modulated by the preparation method. With respect to the wet impregnated samples, cobalt over pure silica, both the amorphous and the ordered MCM-41, are the most active catalysts, with the Co/MCM-41 being the most active, comparable with a traditional CoMo/ASA, and with the smallest initial deactivation. With the increasing content of alumina a decrease of the HDS activity is observed. Conversely, when considering the catalysts prepared by the sodium carbonate method (carb.), opposite trend is obtained, with the silica catalysts being the least active and the alumina containing catalysts the most active. Quite interestingly, comparable activities are obtained for the Co only ASA supported catalyst, prepared by this method, and the more conventional CoMo/ASA catalyst.

Table 1
Thiophene HDS reaction rate (k), apparent activation energy (E_{app}) and percentage of deactivation (d%) of the supported Co catalysts

Sample	r (μmol s^{-1} g^{-1})	E_{app} (kJ/mol)	d (%)
Co/SiO_2 (wi)	0.35	33	28
Co/SiO_2 (carb.)	0.03	n.d	n.d.
Co/ASA (wi)	0.10	n.d.	n.d.
Co/ASA (carb.)	0.35	43	28
$CoAl_2O_3$ (wi)	0.06	–	15
$CoA1_2O_3$ (carb.)	0.23	37	44
Co/S_2 (wi)	0.03	–	–
Co/S_2 (carb.)	0.26	40	19
Co/MCM-41 (wi)	0.42	34	5
Co/MCM-41 (carb.)	0.06	n.d.	n.d.
CoMo/ASA[a]	0.40	85	82
Mo/ASA[a]	0.11	76	n.d

[a] From Ref. [22].

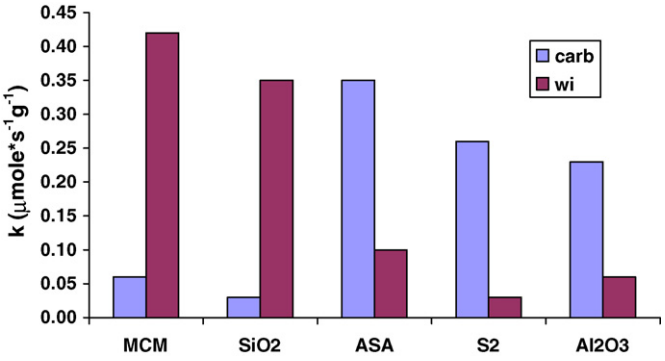

Fig. 1. Variation of the thiophene HDS rate constant with the different supports for the two differently prepared Co catalysts.

In Table 2 the supports with their morphological properties are listed. The support MCM-41 is characterised by the largest surface area and by the narrowest pore size distribution centred at 2.6 nm. The zero point charges, indicative of surface acidity, are all comparable and close to neutral pH except for the more acidic ASA. The XRD patterns, in the 2θ range between 30° and 55°,

Table 2
Surface area (S), average pore diameters (d_p) and zero point charge (ZPC) of the supports

Supports	S (m^2/g)	d_p (nm)	ZPC
SiO_2	316	5.0	6.5
ASA (Al/Si = 0.13)	430	5.0	3.7
S_2 (Al/Si = 2.1)	496	3.5	6.0
$A1_2O_3$	155	12.5	7.0
MCM-41	810	2.6	5.6

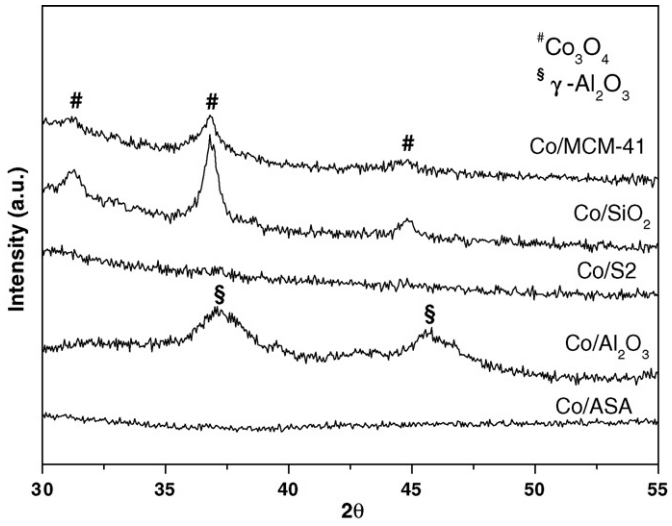

Fig. 2. XRD pattern of calcined supported Co catalysts prepared by wet impregnation.

of the calcined Co catalysts prepared by wet impregnation are shown in Fig. 2. The diffractograms of Co/SiO_2 and Co/MCM-41 catalysts exhibit characteristic XRD lines at $2\theta = 31.3°$, 36.8° and 44.8° of the mixed cobaltous-cobaltic oxide (Co_3O_4) [17]. From the line broadening analyses of the most intense peak, using the Scherrer equation [23], the particle sizes of 15 and 6 nm are obtained respectively for the SiO_2 and the MCM-41 supported catalysts. In the pattern of the Co/Al_2O_3 sample, the presence of the two large bands typical of γ-$A1_2O_3$ located near the 2θ position of the Co_3O_4 peaks, makes difficult the identification of the cobalt oxide. The patterns of the wet impregnated Co/S_2 and Co/ASA are typical of amorphous structure as the starting supports. The XRD patterns (not shown in here) of the corresponding catalysts, obtained with the method of the precipitation with Na_2CO_3 are all similar to the original supports. Therefore, differently from the impregnated samples, the patterns of the Co/SiO_2 (carb.) and Co/MCM-41 (carb.) do not present any diffraction peaks due to crystalline phase. Thus, based on these XRD data, a correlation between the presence of Co_3O_4 species in the calcined samples and the catalytic activity of the silica gel and MCM-41 supported cobalt is envisaged, whereas nothing can be stated about the alumina containing support catalysts. Indeed, the lack of reflection lines in the XRD patterns does not exclude without doubt the presence of crystalline phases at the surface.

Temperature programmed reduction is a powerful mean for the determination of the oxide chemical species. As reported in the literature, the reducibility of cobalt oxide is strongly dependent on the support, loading and promoter effect [9,10,24]. In Figs. 3–5 the TPR profiles of the Co/SiO_2, Co/MCM-41 and Co/Al_2O_3 prepared by the two methods are shown. According to literature [25], unsupported Co_3O_4 contains one or two peaks close to each other in the temperature range of 200–400 °C. The reduction process is assumed to occur in two steps, a lower temperature reduction of Co^{3+} to Co^{2+} and a slightly higher temperature reduction of Co^{2+} to Co^0. Due to a variety of effects such as particle size, morphology, or insufficient hydrogen par-

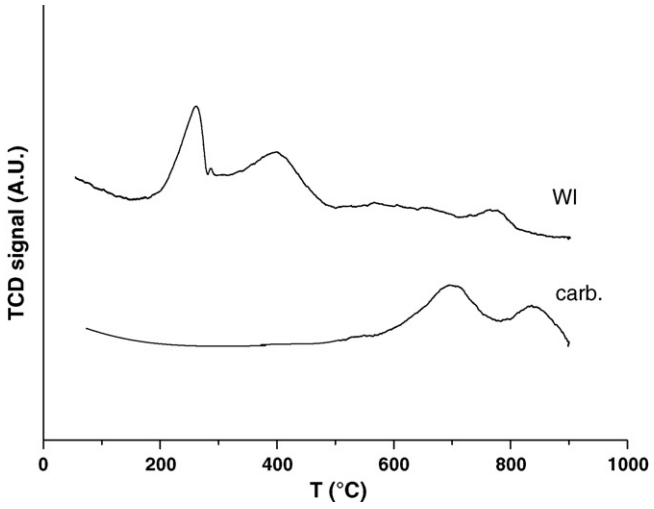

Fig. 3. TPR pattern of Co/SiO_2 catalysts prepared by carbonate and by wet impregnation after calcination.

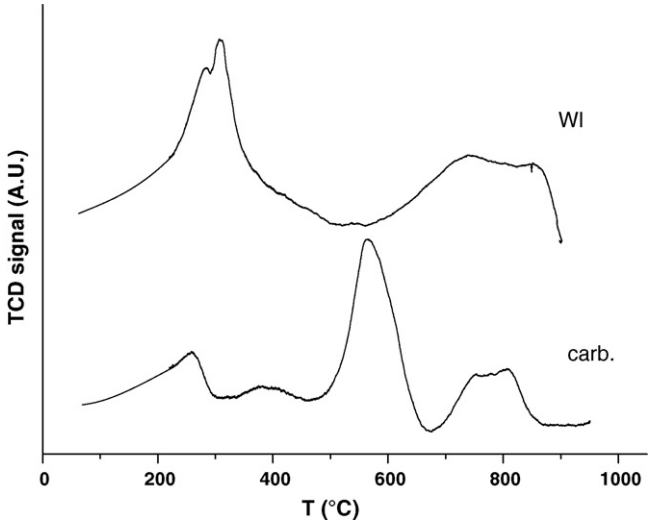

Fig. 4. TPR pattern of Co/MCM-41 catalysts prepared by carbonate and by wet impregnation.

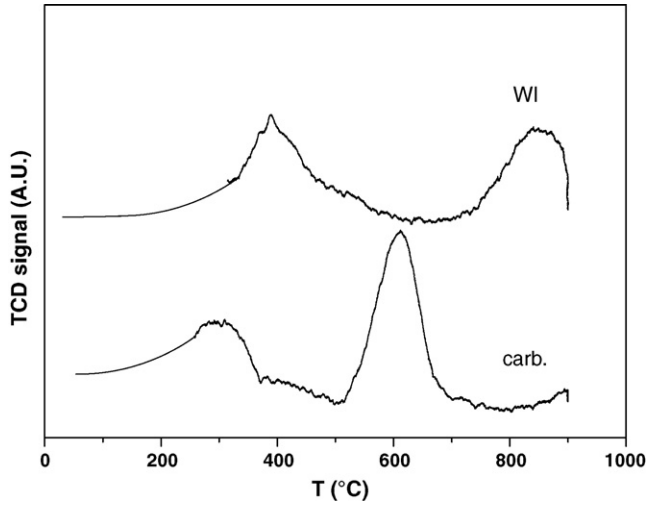

Fig. 5. TPR pattern of Co/Al_2O_3 catalysts prepared by carbonate and by wet impregnation.

tial pressure, the shape of the peaks may not be well defined. As shown in Fig. 3 the reduction profile of Co supported on silica is characterised by two main peaks attributed to the two reduction steps of the Co_3O_4. The small peak at high temperature (~800 °C) could be due to high temperature driven formation of CoO_x–SiO_2 species [24]. The presence of such hard to reduce cobalt species on SiO_2 can also be attributed to Co^{2+} migration into the silica framework [26]. According to the literature the amount of migrating cobalt depends on cobalt dispersion and on the available number of tetrahedral defect sites near the surface for Co^{2+} incorporation. In the case of the Co/SiO_2 samples prepared by precipitation with Na_2CO_3, the high temperature shift of ~400 °C indicates presence of oxide species strongly interacting with the support and therefore more difficult to be reduced. According to literature, stronger Co–SiO_2 interaction may have been created by the basic pH used in the Na_2CO_3 procedure. Indeed, formation of silicates was observed during precipitation of Co/SiO_2 catalysts in alkaline conditions [27]. A reaction between the silic acid (partially dissolved silica) and the cobalt hydroxide formed in basic conditions leads to cobalt silicate embedded into the silica matrix [28]. The TPR pattern of the wet impregnated Co/MCM-41 catalyst (Fig. 4) is characterised by two major features, one at ~300 °C and the other above 700 °C and is similar to the recently reported Co over zirconium-doped mesoporous silica (MSU) [29]. The low temperature peak can be attributed to the unresolved two steps reduction of the Co_3O_4, the high temperature band to the reduction of cobalt species more interacting with the support. According to the literature, higher surface area supports, like MCM-41, are generally more interacting with the supported metal as compared to the lower surface area supports [10,30]. In Fig. 4 the high temperature shift of the main reduction peak of the Na_2CO_3 precipitated Co/MCM-41 sample is shown. The increase in the reduction temperature is again indication of higher interaction with the support probably driven by the alkaline conditions, similarly to the amorphous silica case. As shown in Fig. 5 for the two differently prepared Co/Al_2O_3 catalysts, the reduction profile is also characterised by two large peaks. In this case the reduction behaviour of the impregnated and precipitated catalysts is the reverse of what observed for the silica case. For the impregnated sample the maxima temperatures are much higher with respect to the silica case. The broad low temperature peak is due to the consecutive reduction steps of the Co_3O_4. The peak above 800 °C is attributed to cobalt species strongly interacting with alumina [9,25]. In the case of the precipitated catalyst the TPR peaks shift to lower temperature. The decrease of the reduction temperature is indicative of cobalt oxide species less interacting with the alumina support.

The surface composition and the surface chemical states of the precursor cobalt oxide species were investigated by X-ray photoelectron spectroscopy. In Fig. 6 the Co 2p spectra of the calcined Co catalysts prepared by impregnation of the different supports are shown. The spectra are characterised by the two main spin-orbit components, Co $2p_{3/2}$ and Co $2p_{1/2}$ separated by ~15.5 eV, and by two satellite peaks (shake up) the intensity of which changes with the supports. By curve fitting, a Co $2p_{3/2}$ binding energy at 780.5 eV is obtained for the silica (amorphous

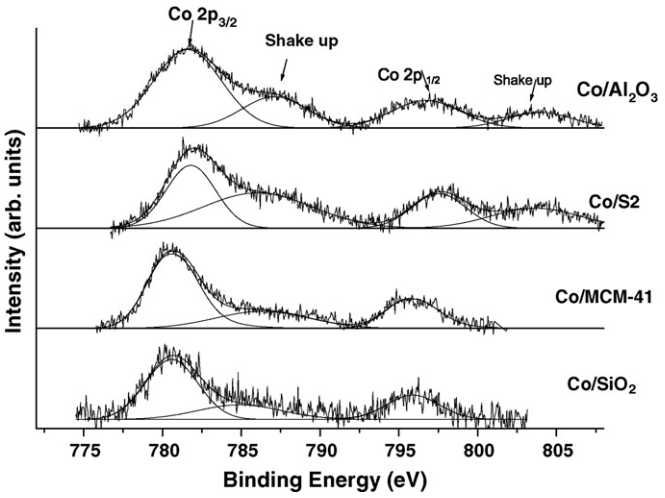

Fig. 6. Co 2p photoelectron spectra of calcined Co supported catalysts prepared by wet impregnation.

SiO_2 and mesoporous MCM-41) supported cobalt. The value is intermediate between the binding energies for Co^{3+} and the Co^{2+} species [31]. In agreement with the XRD data, the spectra are attributed to the Co_3O_4 phase. The Co 2p spectra of the other supported catalysts are characterised by the Co $2p_{3/2}$ = 781.4 eV and by stronger satellite peaks. The high energy shift of the main Co $2p_{3/2}$ binding energy and the increased intensity of the shake up features indicate a greater contribution of Co^{2+} as compared to the Co^{3+} species. These data are in accord with surface Co^{2+} species possibly stabilised by stronger interaction with the alumina containing supports. Co 2p spectra of the catalysts prepared by precipitation with Na_2CO_3 are given in Fig. 7. For the comparison purposes, only the two extreme cases, Co/SiO_2 and Co/Al_2O_3, are shown. By comparing with the spectra of Fig. 6, in the silica supported catalyst the Co $2p_{3/2}$ moves to 781.3 eV along with an increased of the shake up peak intensity whereas in the alumina case the Co $2p_{3/2}$ shifts to 780.5 eV with a decrease of the satellite peak. In agreement with the disappearance of the XRD Co_3O_4 reflections for the silica samples and with the shift of the TPR peaks for the silica and alumina catalysts, a reversal of the chemical state of cobalt takes place. With the precipitation procedure, more of Co^{2+} interacting with the support is formed

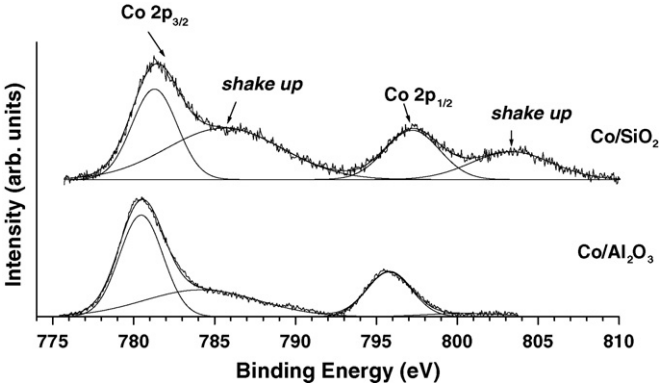

Fig. 7. Co 2p photoelectron spectra of Co/SiO_2 and Co/Al_2O_3 catalysts prepared by carbonate.

Table 3
XPS data after sulfiding with H_2/H_2S (sulf) and after being used in the catalytic reaction (aged)

Sample	Co $2p_{3/2}$		S/Co at		Co/Si	
	Sulf[a]	Aged[a]	Sulf	Aged	Sulf[b]	Aged
Co/SiO_2	778.5 (33) 781.6 (67)	778.1 (20) 781.5 (80)	0.2	0.9	0.01 (0.01)	0.005
Co/MCM	779.1 (20) 781.5 (80)	778.3 (20) 782.1 (80)	0.2	1.1	0.04 (0.01)	0.01

[a] Values in parentheses are the relative percentage of each Co $2p_{3/2}$ component.
[b] For comparison reason the values of the calcined samples are given in parentheses.

on the surface of the SiO_2 and more of Co_3O_4 is formed on Al_2O_3.

From the above-described results, an activity–oxide structure relationship is inferred. In order to investigate the modification undergone by the catalyst through the various stages of its life, the XPS analyses of the sulfided and used catalysts were performed and compared with corresponding analyses of the calcined samples. Only the most active silica supported catalysts were explored in details. In Table 3 the S 2p and the Co 2p binding energies, with the components signal percentages in parentheses, after sulfiding with H_2/H_2S (sulf) and after being used in catalysis (aged) are listed along with corresponding XPS derived atomic ratios S/Co and Co/Si. In Figs. 8 and 9 the Co $2p_{3/2}$ spectra of the Co/SiO_2 and Co/MCM-41 catalysts after the different treatments are shown respectively. The Co $2p_{3/2}$ spectra of the pre-treated catalysts can be decomposed into two peaks, one due to metal sulfide and the other to oxidic cobalt(II). In fact, the low binding energy peak at 778.8 ± 0.4 eV can be attributed to cobalt sulfide or to cobalt metal, since they are undistinguishable. The binding energy of the Co $2p_{3/2}$ level in Co metal is indeed close to that in Co_9S_8 and both species do not show any characteristic satellite structure [10,30]. Moreover, detection of a broad S 2p signal at ~162 eV with the atomic ratio S/Co (considering only the Co 2p component at 778.8 eV) approximately close to 1 suggests formation of the thermodynamically favoured Co_9S_8 [32]. The high energy peak at 781.5 ± 0.1 eV with a rather broad satellite feature in the range of 785–787 eV is attributed to Co(II). It is worth noticing in Figs. 8 and 9 and in Table 3 that the relative amount of the low binding energy Co 2p component after the H_2/H_2S treat-

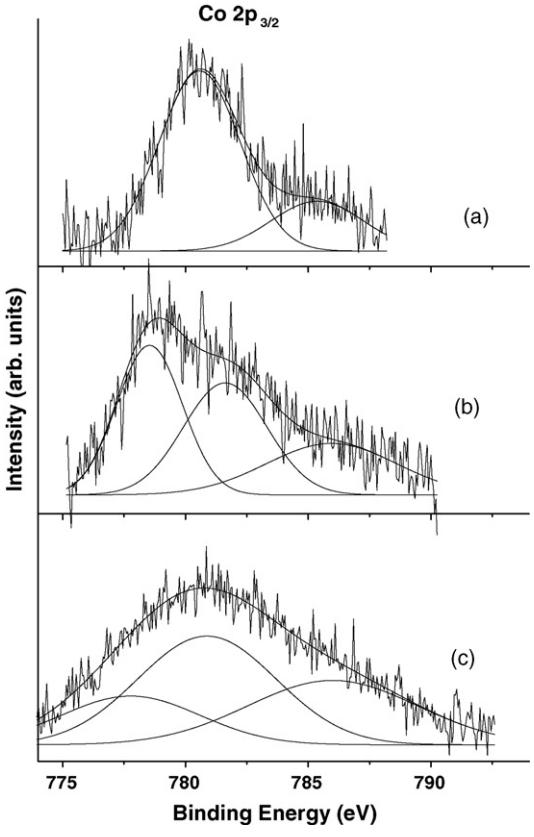

Fig. 8. Co $2p_{3/2}$ photoelectron spectra of Co/SiO_2 (a) calcined; (b) after pre-treatment with H_2/H_2S; (c) after HDS reaction.

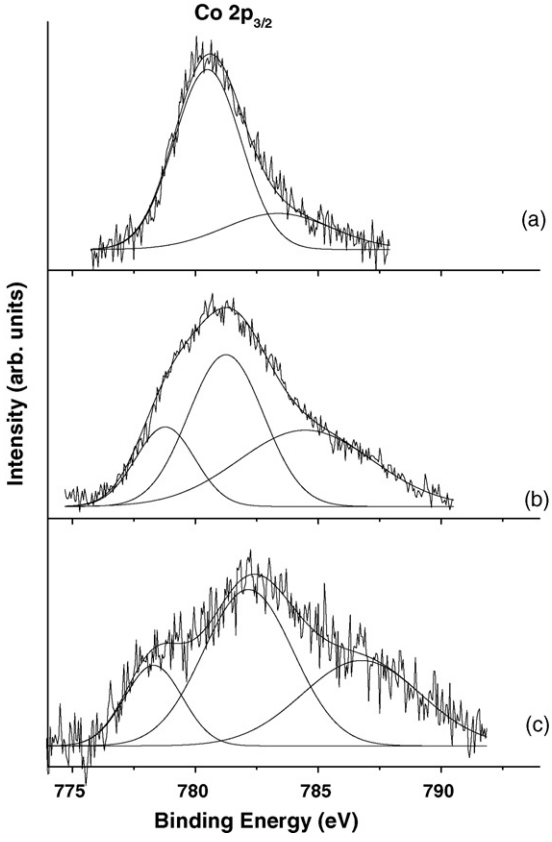

Fig. 9. Co $2p_{3/2}$ photoelectron spectra of Co/MCM-41 (a) calcined; (b) after pre-treatment with H_2/H_2S; (c) after HDS reaction.

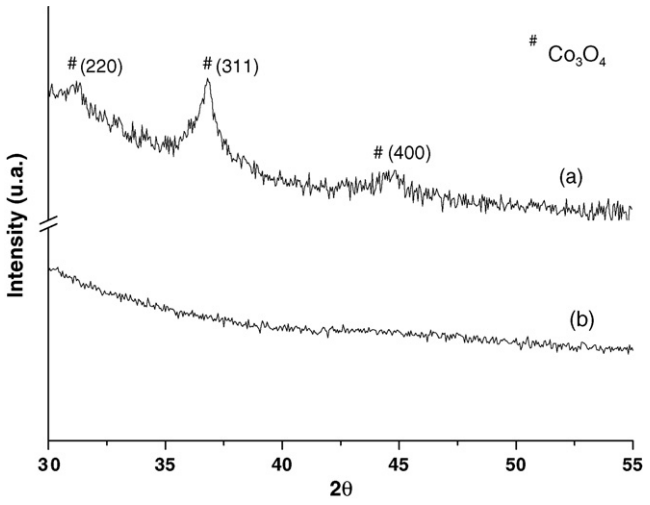

Fig. 10. XRD patterns of Co/MCM-4 as (a) calcined; (b) pre-treated with H_2/H_2S.

ment is lower in the MCM-41 catalyst as compared to the SiO_2 one. This results is in accord with the TPR profiles consistent with more hardly reducible cobalt species being formed in the Co/MCM-41. The Co/Si ratios of the calcined samples are given in parentheses in Table 3. It is worth noticing the increased ratio obtained for the Co/MCM-41 after the treatment with H_2/H_2S. Such increase, with respect to the only calcined sample, indicates a re-dispersion of the cobalt on the surface of the support, probably favoured by the morphology and by the more chemically interacting structure of the mesoporous support. The effect of the sulfiding treatment is also observed in the corresponding XRD pattern shown in Fig. 10. The disappearance of the Co_3O_4 reflection peaks and the lack of any sulfide related peaks are in agreement with an increased cobalt species dispersion. Such high cobalt dispersion, along with the initially smaller Co_3O_4 particle size, could explain the larger activity of the Co/MCM-41 (wi) as compared to the Co/SiO_2 (wi) in spite of its lower reducibility.

The incomplete sulfidation of the Co species, ascribed to H_2S diffusion limitation in the large size Co_3O_4 particle [33] does not appear to be a drawback for the catalytic activity. Indeed, as recently reported for CoMo catalysts, besides the reducibility and the active species dispersion, an important role in HDS activity is played by a low state of sulfidation of the Co species with specific electronic properties due to the presence of oxidised Co ions [34]. A synergy between the Co_9S_8 and the CoO may occur. As reported for some supported CoMo systems, the sulfur vacancies of the Co_8S_9 may serve as activation sites for the thiophene [35] and the cobalt oxide as activation sites for the H_2 [36]. From the XPS analyses of the catalyst after reaction, the surface atomic ratio Co/Si, as shown in Table 3, decreases noticeably. At the same time the XPS atomic ratio of sulfur to total cobalt increases up to a value of 1. Moreover as shown from Figs. 8(c) and 9(c), the relative peak intensity of Co 2p(Co_9S_8)/Co 2p(Co^{2+}) does not change in the Co/MCM-41, whereas it decreases in the Co/SiO_2 catalyst, in agreement with the better initial stability of the MCM-41 supported catalyst (Table 1). The deterioration of the Co 2p signal along with the decrease of the XPS atomic ratio Co/Si after reaction may be attributed to some preferential coke or sulfur species deposition. Further studies on the catalyst deactivation are in progress.

4. Conclusion

The main result of this study is the possibility of reversing the support effect by changing the synthesis procedure. Such approach allows to establish the Co_3O_4 as the active oxide precursor in the cobalt based HDS catalysts. Regardless the type of support, very interacting like alumina or inert like silica, it is possible through appropriate Co-supporting methods to favour the formation of such species. Quite interestingly, supported Co only catalyst with activity comparable to the corresponding CoMo catalyst is obtained. Moreover, the smaller Co_3O_4 particle size of the calcined sample and the increased dispersion of Co species upon H_2/H_2S treatment account for the superior activity of Co/MCM-41 (wi) as compared to the Co/SiO_2 (wi).

Acknowledgements

Support by European Community, Network of Excellence (NoE) IDECAT (Integrated Design of Catalytic Nanomaterials for Sustainable Production) and COST D36 action is acknowledged.

References

[1] K.G. Knudsen, B.H. Cooper, H. Topsøe, Appl. Catal. A 189 (1999) 205.
[2] H. Topsøe, B.S. Clausen, F.E. Massoth, in: J.R. Anderson, M. Boudart (Eds.), Springer-Verlag, Berlin, 1996.
[3] R.J.H. Voorhoeve, J. Catal. 23 (1971) 236.
[4] P. Grange, B. Delmon, J. Less-Common Met. 36 (1974) 353.
[5] N.-Y. Topsøe, H. Topsøe, J. Catal. 84 (1983) 386.
[6] J.P.R. Vissers, V.H.J. de Beer, R. Prins, J. Chem. Soc. Faraday Trans. 1 (83) (1987) 2145.
[7] Y. Minato, A. Kuriko, S. Masayuki, A. Masahiko, Appl. Catal. A 209 (2001) 79.
[8] E. Hayashi, E. Iwamatsu, M.E. Biswas, Y. Sanada, S. Ahmed, H. Hamid, T. Yoneda, Appl. Catal. A 179 (1999) 203.
[9] M. Vofi, D. Borgmann, G. Wendler, J. Catal. 212 (2002) 10.
[10] L.B. Backman, A. Rautiaien, M. Lindblad, O. Jylha, A.O.I. Krause, Appl. Catal. A 208 (2001) 223.
[11] V. La Parola, G. Deganello, A.M. Venezia, Appl. Catal. A 260 (2004) 237.
[12] B. Scheffer, P. Arnoldy, J.A. Moulijn, J. Catal. 112 (1988) 516.
[13] V. La Parola, G. Deganello, S. Scire, A.M. Venezia, Solid State Chem. 174 (2003) 482–488.
[14] J. Choma, S. Pikus, M. Jaroniec, Appl. Surf. Sci. 252 (2005) 562.
[15] A. Corma, A. Martinez, V. Martinez-Soria, J. Catal. 169 (1997) 480.
[16] A. Wang, Y. Wang, T. Kabe, Y. Chen, A. Ishihara, W. Quian, J. Catal. 199 (2001) 19.
[17] JCPDS Powder Diffraction File, International Centre for Diffraction Data, Swarthmore, File No. 42-1467.
[18] S.J. Gregg, K.S. Sing, Adsorption, Surface Area and Porosity, 2nd ed., Academic Press, San Diego, 1982.
[19] D.A. Shirley, Phys. Rev. B5 (1972) 4709.
[20] P.M.A. Sherwood, in: D. Briggs, M.P. Seah (Eds.), Practical Surface Analysis, Wiley, New York, 1990, p. 181.
[21] S. Subramanian, J.S. Noh, J.A. Schwarz, J. Catal. 114 (1988) 433.
[22] A.M. Venezia, F. Raimondi, V. La Parola, G. Deganello, J. Catal. 194 (2000) 393.

[23] H.P. Klug, X-Ray Diffraction Procedure for Polycrystalline and Amorphous Materials, Wiley, New York, 1954.
[24] G. Jacobs, T.K. Das, Y. Zhang, J. Li, G. Racoillet, B.H. Davis, Appl. Catal. A 233 (2002) 263.
[25] R.L. Chin, D.M. Hercules, J. Phys. Chem. 86 (1982) 3079.
[26] K.E. Coultier, A.G. Sault, J. Catal. 154 (1995) 56.
[27] I. Puskas, T.H. Fleish, J.B. Hall, B.L. Meyers, R.T. Roginski, J. Catal. 134 (1992).
[28] I. Puskas, T.H. Fleisch, P.R. Full, J.A. Kaduk, C.L. Marshall, B.L. Meyers, Appl. Catal. A 311 (2006) 146.
[29] A. Infantes-Molina, J. Merida-Robles, E. Rodriguez-Castellon, J.L.G. Fierro, A. Jimenez-Lopez, J. Catal. 240 (2006) 258.
[30] J. Panpranot, J.G. Goodwin Jr., A. Sayari, Catal. Today 77 (2002) 269.
[31] M.A. Stranick, M. Houalla, D.M. Hercules, J. Catal. 103 (1987) 151.
[32] Y. Okamoto, T. Imanaka, S. Teranishi, J. Catal. 85 (1980) 448.
[33] K. Inamura, T. Takyu, Y. Okamoto, K. Nagata, T. Imanaka, J. Catal. 133 (1992) 498.
[34] T.A. Sepeda, J.L.G. Fierro, B. Pawelec, R. Nova, T. Klimova, G.A. Fuentes, T. Halachev, Chem. Mater. 17 (2005) 4062.
[35] R.G. Leliveld, A.J. van Dillen, J.W. Geus, D.C. Koningsberger, J. Catal. 175 (1998) 108.
[36] R.I. Declerck-Grimes, P. Canesson, R.M. Friedman, J.J. Fripiat, J. Phys. Chem. 82 (1978) 889.